The American Journal of Pathology, Vol. 181, No. 2, August 2012

http://dx.doi.org/10.1016/j.ajpath.2012.04.021

Metabolic, Endocrine, and Genitourinary Pathobiology

Global Levels of H3K27me3 Track with Differentiation *in Vivo* and Are Deregulated by MYC in Prostate Cancer

Laxmi G. Pellakuru,* Tsuyoshi Iwata,* Bora Gurel,* Denise Schultz,* Jessica Hicks,* Carlise Bethel,* Srinivasan Yegnasubramanian,†‡ and Angelo M. De Marzo*†‡§¶

From the Departments of Pathology, Oncology,† and Urology,§ the Sidney Kimmel Comprehensive Cancer Center at Johns Hopkins,‡ and the Brady Urological Research Institute,¶ The Johns Hopkins University School of Medicine, Baltimore, Maryland*

Cancer cells and stem cells share a number of biological characteristics including abundant amounts of decondensed chromatin. However, the molecular correlates and the factors involved in altering chromatin structure in cancer cells are not well known. Here, we report that less differentiated stem-like cells in the basal compartment of human and mouse prostate contain lower levels of the polycomb heterochromatin marker H3K27me3 than more differentiated luminal cells. This link to differentiated normal cells is also found in a number of other human and rodent tissues characterized by hierarchical differentiation. In addition to MYC's traditional role as a gene-specific transcription factor, recent studies indicate that MYC also affects global chromatin structure where it is required to maintain "open" or active chromatin. We now demonstrate that in both MYC-driven prostate cancers in mice and human prostate cancers, global levels of H3K27me3 are reduced in prostatic intraepithelial neoplasia and invasive adenocarcinoma lesions. Moreover, decreased levels of H3K27me3 correlate with increased markers of disease aggressiveness (eg, Gleason score and pathological stage). *In vitro*, experimentally forced reductions in MYC levels result in increased global levels of H3K27me3. These findings suggest that increased levels of decondensed chromatin in both normal progenitor cells and cancer cells are associated with global loss of H3K27me3, which is linked to MYC overexpression. ***(Am J Pathol 2012, 181:560–569; http://dx.doi.org/10.1016/j.ajpath.2012.04.021)***

Cancer cells and embryonic stem cells (ESCs) share a number of biological features including a block in terminal differentiation and the capacity for unlimited self-renewal. One potential link between stem cells and cancer is the potent oncogene *MYC*. MYC is a sequence-specific transcription factor that is overexpressed in up to 70% of all human cancers and regulates a large number of cellular processes, including DNA replication, ribosome biogenesis and mitochondrial function.[1] MYC is required for embryonic development as well as maintenance of ESC self-renewal.[2,3] Further, *MYC* is one of four genes required for efficient epigenetic reprogramming of adult differentiated cells into induced pluripotent stem cells (iPSCs),[4,5] which share virtually all of the biological properties of ESCs. Additionally, many human cancers express transcriptional programs that are characteristic of a "MYC" signature, and this signature is highly active in ESCs.[6–8]

In addition to the classical view that MYC functions primarily by controlling the transcription of specific genes, another feature that appears to link MYC to stem cells and cancer cells is its ability to regulate global chromatin structure.[9] It is well known that stem cells and progenitor cells are characterized by an "open" conformation that consists predominantly of decondensed euchromatin with

Supported by the Patrick C. Walsh Prostate Cancer Fund, of which A.M.D.M. is the Peter J. Sharp Scholar, Prostate SPORE P50CA58236, and a research award from Mr. David Koch.

Accepted for publication April 12, 2012.

Disclosures: A.M.D.M. is currently employed at Predictive Biosciences, Inc. (Lexington MA), as well as part-time adjunct Professor of Pathology, Oncology, and Urology at the Johns Hopkins University School of Medicine (Baltimore, MD). No funding or other support was provided by Predictive Biosciences, Inc., for any of the work in this manuscript. The terms of the relationship between A.M.D.M. and Predictive Biosciences, Inc., are managed by the Johns Hopkins University in accordance with its conflict-of-interest policies.

Supplemental material for this article can be found at *http://ajp.amjpathol.org* or at *http://dx.doi.org/10.1016/j.ajpath.2012.04.021*.

Address reprint requests to Angelo M. De Marzo, M.D., Ph.D., Koch Cancer Research Building, Rm. 142, 1550 Orleans St., Baltimore, MD 21231. E-mail: ademarz@jhmi.edu.

little condensed heterochromatin.[10] Interestingly, MYC family members can regulate global chromatin openness and accessibility. For example, Knoepfler et al[11] found that deletion of *Nmyc* (alias N-myc) in developing cerebellar granule neural progenitors (CGNPs) resulted in loss of open chromatin and a premature nuclear chromatin condensation. These changes were characterized by decreased levels of acetylation of histones H3 and H4, modifications generally associated with open and active chromatin. In terms of histone tail methylation, Knoepfler et al found that *Nmyc*-null CGNPs exhibited high levels of H3K9me2 and H3K9me3, both of which are associated with repressive heterochromatin, and a reduction in H3K4me3, which is associated with active euchromatin.[11] These findings, along with other recent genome-wide studies, which document widespread MYC binding and influence on global levels of histone modifications, support the emerging concept that a novel mechanism by which MYC overexpression can influence cellular properties involves changes to overall chromatin organization and structure.[3,12,13]

It has been well known that many cancer types contain a relatively large fraction of cells that possess decondensed "open" or "vesicular" chromatin, and this feature is often helpful in establishing the diagnosis of cancer by pathologists.[14,15] Prostate cancer develops from intraepithelial lesions referred to as prostatic intraepithelial neoplasia (PIN). PIN and prostate cancer cells, like many other cancer types, are characterized by enlarged nuclei with increased amounts of decondensed "open" chromatin and prominent enlarged nucleoli.[16–18] Recently, it has become clear that in addition to MYC's long-suspected role in prostate cancer progression (as a result of gain of chromosome 8q24), human PIN, and cancer lesions very commonly overexpress MYC protein even in the absence of 8q24 gain.[19,20] Further, in transgenic mice programed to overexpress MYC in the prostate, the onset of MYC overexpression corresponds precisely with the onset of nuclear enlargement, nucleolar enlargement, increased numbers of nucleoli, and global chromatin decondensation.[16] Given MYC's new and unexpected role in influencing global chromatin structure, we have begun to investigate whether the extent of global levels of well-studied posttranslational histone modifications within chromatin are altered during prostatic carcinogenesis and whether MYC overexpression results in alterations in global levels of such modifications in human and mouse prostate PIN and cancer lesions.

One well-known posttranslational modification of histone tails that is tightly regulated in development and during ESC differentiation is the polycomb mark trimethylation of histone H3 on lysine 27 (H3K27me3). This mark is generally associated with transcriptional repression, a closed heterochromatic structure, and dysregulation in a number of cancers. For example, in myelodysplastic syndrome,[21] recent studies have identified inactivating mutations in the H3K27me3 methyltransferase enhancer of zeste homolog 2 (EZH2), which is the catalytic subunit of the polycomb repressive complex 2 (PRC2). Although global levels of H3K27me3 have not been previously studied in the setting of EZH2 mutations in myelodysplastic syndrome, the presence of EZH2 mutations suggests that loss of H3K27me3, perhaps in specific loci, is important in this disease.[22] EZH2 mutations also occur in some diffuse large cell lymphomas, as well as some follicular lymphomas, and in these diseases, it remains somewhat controversial whether the mutations are inactivating or activating.[23–25] In contrast to these results suggesting that EZH2 functions as a tumor suppressor in myelodysplastic syndrome, and unclear results in lymphoma, EZH2 has been shown more clearly to have an oncogenic role in a number of other cancer types. For example, overexpression of wild-type EZH2 has been documented in breast and prostate cancer.[26–28] Further, forced overexpression of EZH2 can transform prostatic epithelial cells *in vitro*[29]; forced reductions in EZH2 decrease prostate and breast cancer cell proliferation.[26,28,30,31] Furthermore, a PRC2 target gene signature is predictive of poor outcome in prostate cancer.[23]

Despite an apparent increase of H3K27me3 in the promoter regions of specific genes in prostate and breast cancer, reductions in global levels of H3K27me3 have been reported to occur in cancers of the breast, pancreas, ovary, and kidney, as compared to levels found in their normal tissues.[32,33] However, there is still much to be learned about the global levels of H3K27me3 and about the mechanisms by which these levels can become altered during normal differentiation and carcinogenesis. In the present study, we used immunohistochemical (IHC) and multilabel immunofluorescent staining to probe global H3K27me3 levels in various normal human and mouse tissue samples, in human prostate cancer and precursor lesions, as well as in MYC-driven mouse PIN and adenocarcinoma lesions. Further, to begin to gain mechanistic insights into regulation of global H3K27me3 levels, we asked whether forced reductions in MYC resulted in changes in global H3K27me3 levels.

Materials and Methods

Western Blot Analysis

For Western blotting of non-histone proteins, cells were lysed in radioimmunoprecipitation assay buffer. Lysates were then centrifuged at 14,000 × *g* for 10 minutes at 4°C. For Western blotting of histone proteins, cells were lysed in triton extraction buffer then dialyzed into 0.01 mol/L trichloroacetic acid (yield: purified histone proteins). Proteins were electrophoresed and transferred to nitrocellulose membranes for immunoblotting. Membranes were probed with the antibodies as follows: MYC (#1472-1, 1:5000 dilution; Epitomics, Burlingame, CA); tubulin (CP06, 1:2000; Calbiochem, Gibbstown, NJ); histone H3 (#39163, 1:10,000 dilution; Active Motif, Carlsbad, CA); H3K27me3 (#39155, 1:2000 dilution; Active Motif); and androgen receptor (AR) (sc-816, 1:2000 dilution; Santa Cruz Biotechnology, Santa Cruz, CA). The blots were quantitatively analyzed using the Odyssey Infrared Imaging System (LI-COR Biosciences, Lincoln, NE) and R statistics package.

Immunohistochemistry

Immunohistochemistry was performed using the Power Vision+ Poly-HRP IHC Kit (ImmunoVision, Springdale, AZ). Slides were steamed for 40 minutes in EDTA solution (Zymed Laboratories/Invitrogen, Carlsbad, CA) and incubated with rabbit polyclonal anti-histone H3 antibody (1:4000 dilution) for 45 minutes, rabbit polyclonal anti–c-MYC antibody (1:300) overnight at 4°C, or mouse monoclonal anti-H3K27me3 (ab6002, 1:200; Abcam, Cambridge, MA) overnight at 4°C. Poly-HRP–conjugated anti-mouse/rabbit IgG antibody was used as secondary antibody. Staining was visualized using 3,3′-diaminobenzidine (Sigma, St. Louis, MO), and slides were counterstained with hematoxylin.

Immunofluorescence

Pretreatment conditions and primary antibody dilutions for histone H3 and H3K27me3 were the same as for immunohistochemistry. Slides were incubated with rabbit polyclonal cytokeratin 5 antibody (PRB-160P, 1:15000; Covance, Princeton, NJ) for 45 minutes. The immunocomplexes were labeled with secondary antibodies conjugated with Alexa 488 or Alexa 568 dyes (Invitrogen), and nuclei were counterstained with DAPI. Slides were visualized using a Nikon E400 fluorescence microscope (Nikon Instruments, Melville, NY).

Cell Culture

The human prostate cancer cell lines LNCaP, DU145, and PC3 and the human breast cancer cell line MCF7 were obtained from the ATCC (Rockville, MD). p493 cells were a generous gift from Chi Van Dang (Johns Hopkins, Baltimore MD). All cells were maintained at 37°C and 5% CO_2, and supplemented with RPMI 1640 or Dulbecco's modified Eagle's medium with 10% serum.

Transfections

Cells were transfected using Oligofectamine or Lipofectamine 2000 (Invitrogen). Pools containing four small-interfering RNA (siRNAs) against MYC (L-003282; Dharmacon, Lafayette, CO) or against AR (L-003400; Dharmacon) were transfected at a final concentration of 50 nmol/L. As a control in each transfection experiment, cells were transfected with siCONTROL Non-Targeting siRNA Pool #1 (D-001810; Dharmacon).

Tissues and Tissue Microarrays

This study was approved by the Johns Hopkins University School of Medicine institutional review board. TMAs were constructed and evaluated as described.[19]

Analysis of Immunohistological Staining

Each scanned image from the TMAs was re-diagnosed by B.G., and regions of interest were demarcated for semiquantitative image analysis using FrIDA as described.[19] Briefly, for brown staining, we determined the median intensity of staining as well as the area of nuclear staining. Since H3K27me3 IHC staining was localized exclusively to nuclei, we derived the percentage of nuclear area staining in regions of interest by dividing the total area of brown staining by the total area of brown plus blue (hematoxylin) staining. We also derived an H3K27me3 score by summing all brown staining in the region of interest and dividing that by the area of brown plus blue staining. Statistical analyses for TMA data were performed using R.

Results

H3K27me3 Levels Are Reduced in Stem/Progenitor Cell Compartments in Multiple Human and Mouse Tissues

Normal prostatic epithelial cells generally showed intense positive staining for H3K27me3 in nuclei within the luminal compartment. Conversely, basal cells (highlighted by keratin 5 staining in Figure 1, A–D), which are thought to be stem-like cells and known to be less differentiated than luminal cells,[34,35] showed markedly less staining for H3K27me3 than the luminal cells. Staining for total H3 protein showed similar levels in prostate basal and luminal cells (Figure 1, E–H; see also Supplemental Figure S1 at *http://ajp.amjpathol.org*), indicating that the difference in basal cell versus luminal cell staining for H3K27me3 is likely not the result of antigen inaccessibility to the antibody. Also, levels of H3K4me3, generally known as an activation mark found predominantly in euchromatin, also did not appear different between basal versus luminal cells (not shown). These results indicate that H3K27me3 levels correlate with differentiation in the human prostate. Similar results showing strong luminal cell staining and weak basal cell staining were seen in the mouse prostate (Figure 2, A and B).

To determine whether global H3K27me3 levels correlate with cellular differentiation status beyond the prostate, we performed immunostaining across a variety of normal tissues. Interestingly, rapidly renewing epithelial tissues that display hierarchical differentiation were generally found to have H3K27me3 staining patterns that correlated directly with increasing degrees of differentiation. Crypts in the small intestine and colon (Figure 3, A and B), where stem cells are localized, showed little to no H3K27me3, whereas the cells in the more differentiated areas toward the luminal surface showed higher amounts of H3K27me3 staining. Similarly, in the mouse tongue, which is characterized by a stratified squamous epithelium, H3K27me3 levels were higher in the more differentiated cells toward the surface as compared to the stem-like cells in the basal compartment (Figure 3C). Conversely, in tissues that do not rapidly renew and that do not show hierarchal differentiation patterns (eg, kidney, liver, pancreas, lung, salivary gland, thyroid; see Supplemental Figure S2, A–F, at *http://ajp.amjpathol.org*), there was little variation in H3K27me3 staining levels ac-

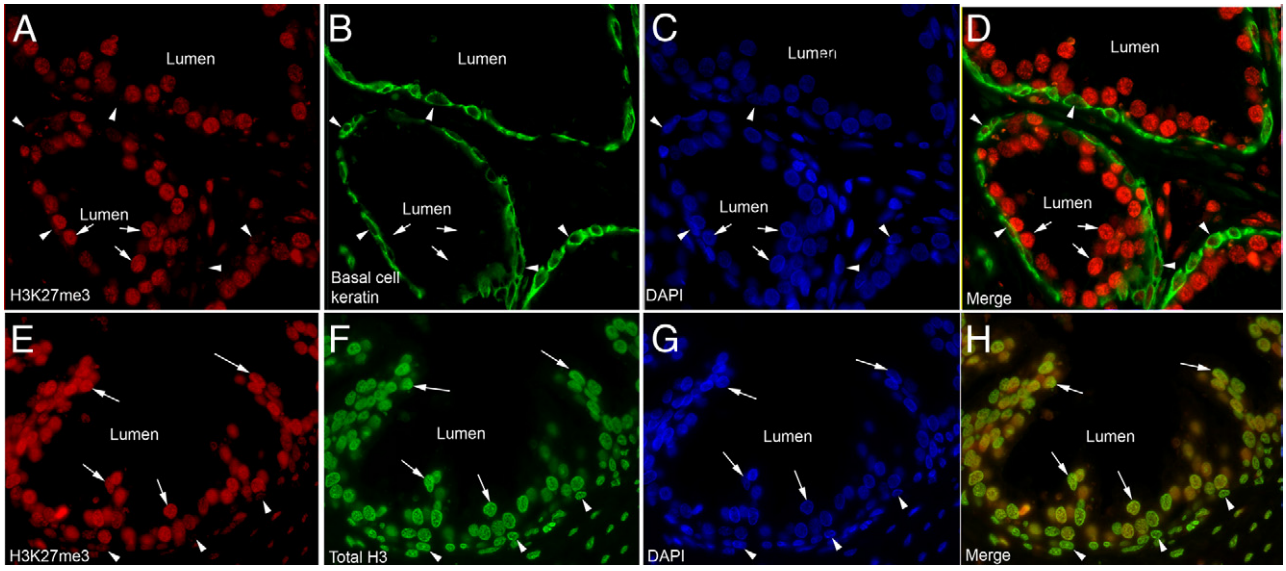

Figure 1. H3K27me3 levels correlate with differentiation in human prostatic epithelium. **A–D:** Immunofluorescence (IF) staining of H3K27me3 and a basal cell cytokeratin (keratin 5) shows a decrease in levels of H3K27me3 in basal cells (**arrowheads**) as compared to luminal cells (**arrows**). **E–H:** This decrease is independent of levels of total histone H3 as they are similar in both luminal and basal cells. Nuclei are counterstained with DAPI.

cording to cell type or location within the tissue, although there was low staining in the germinal center of lymphoid tissue in the tonsil (see Supplemental Figure S2F at *http://ajp.amjpathol.org*). Similar findings of generalized increases in H3K27me3 with differentiation in tissues showing rapid turnover and hierarchical differentiation, with more homogeneous staining in tissues without apparent hierarchical differentiation, were found in both mouse and rat tissues (not shown). Taken together, these data indicate that H3K27me3 staining levels correlate with the degree of differentiation/maturation across a number of organ systems and suggest the potential for H3K27me3 staining to serve as a biomarker of terminal differentiation (eg, increasing levels of staining occur as cells differentiate/mature).

H3K27me3 Levels Are Reduced in Inflammation-Associated, Preneoplastic, and Neoplastic Lesions of the Prostate

We next examined H3K27me3 staining in different prostatic lesions using tissue microarrays (Tables 1 and 2). A subset of prostatic atrophy lesions have been shown previously to harbor some of the characteristic molecular alterations of PIN and prostatic adenocarcinoma including hypermethylation of the *GSPT1* upstream promoter/CpG island; these lesions have been found in association with PIN and early adenocarcinoma lesions.[36] Interest-

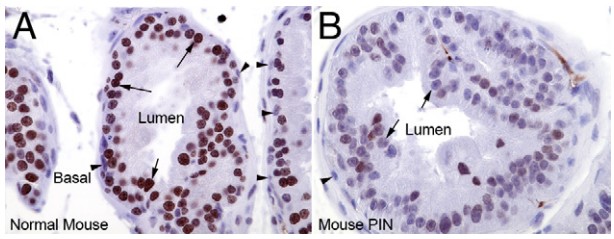

Figure 2. H3K27me3 levels are reduced in mouse MYC-driven PIN lesions. As compared to normal mouse prostate (**A**), H3K27me3 levels are reduced in mouse PIN lesions (**B**). **Arrows** indicate luminal cells. **Arrowheads** indicate basal cells. Original magnification, ×400.

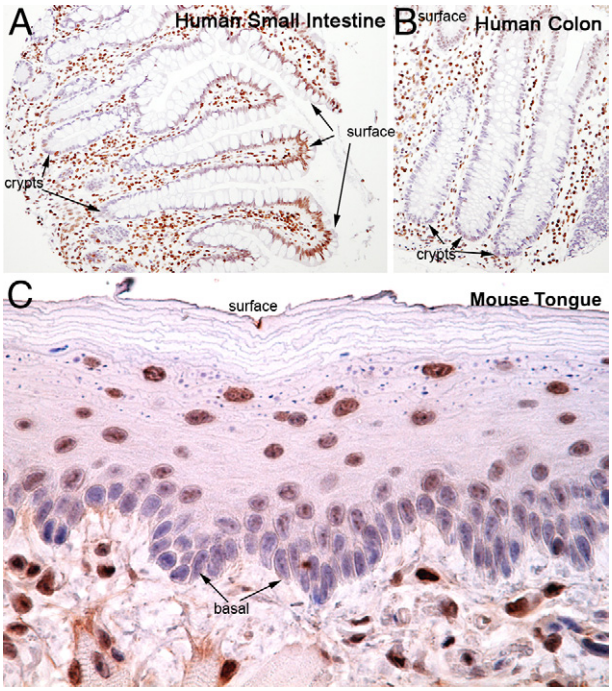

Figure 3. H3K27me3 levels correlate with differentiation in numerous tissues. Immunohistochemical staining of human small intestine (**A**) and colon (**B**) demonstrating that H3K27me3 staining is very low in the crypts, which harbor the stem-like and less differentiated cells, and increases in the more differentiated cells toward the lumen. Original magnification, ×200. **C:** This observation is also seen in mouse tissues including the mouse tongue (original magnification, ×400). Less differentiated basal-most cells show much weaker staining for H3K27me3 as compared to more mature cells closer to the surface (top of image).

Table 1. Pathological Features of Radical Prostatectomy Cases Used in This Study on TMAs

	Pathological stage			
Gleason score	T2	T3A	T3B	Total
5 to 6	39	9	1	49
7	9	21	14	44
8 to 9	4	26	31	61
Total	52	56	46	154

Fisher's exact test, $P < 0.001$.

ingly, there is reduced luminal cell staining in many prostatic atrophy lesions in which a fraction of the cells express both "basal cell–specific" and luminal-enriched keratins at high levels as well as variable levels of differentiation markers such as NKX3.1, AR, and prostate-specific antigen (PSA). Thus, these lesions are enriched for cells possessing a phenotype intermediate between basal and luminal cells (Figure 4, A–F, Table 2). Our chromogenic image analysis approach allows us to examine both the intensity of staining (median intensity was used) as well as the area of staining within given tissues. In atrophy, although the overall area of staining was significantly reduced compared to normal epithelium (ie, area of brown nuclear staining over total nuclear area), the median intensity of those cells staining positively was not significantly reduced.

Strikingly, most cases of prostatic intraepithelial neoplasia (PIN), which is considered a key direct precursor to human prostatic adenocarcinoma, showed markedly reduced immunostaining in many of the neoplastic luminal cells as compared with benign, normal-appearing luminal cells from the same cases (Figures 4 and 5). In PIN, both the median intensity and area of staining were

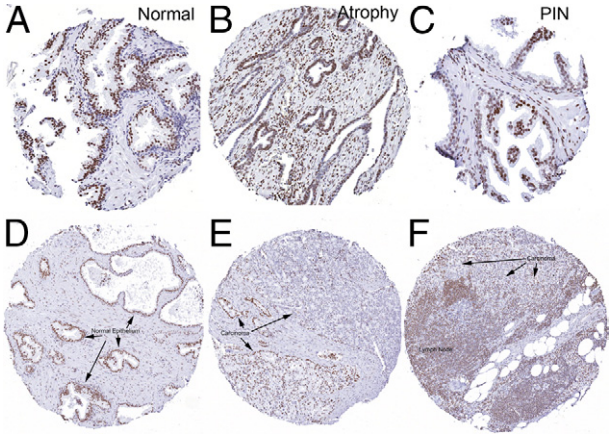

Figure 4. H3K27me3 levels are reduced in atrophy, PIN, and cancer. Representative immunohistochemical staining of normal prostate tissue (**A** and **D**) (**arrows** indicate normal epithelium), focal atrophy (**B**), and PIN (**C**). Note decreased staining atrophy and PIN compared with normal. Staining in primary carcinoma (**E**) and a lymph node metastasis (**F**) shows decreased staining for H3K27me3 in the tumor tissue as compared to the normal (**arrows** indicate carcinoma). **D** and **E** are from the same patient. Original magnification, ×200.

reduced. Interestingly, the PIN cells located most closely to the basement membrane tended to show less staining for H3K27me3 than cells located toward the tips of papillae toward the lumen.

We next examined prostatic adenocarcinoma lesions and found reduced staining, as compared to normal matched luminal cells, in the majority of cases (Figures 4 and 5). Most carcinomas showed variable staining with some cells staining strongly positive and others with reduced and markedly reduced staining. Despite this variability, there was a progressive decrease in both median intensity and area of nuclear staining with increasing

Table 2. Histopathology of TMA Scores Evaluated by Automated Image Analyses for H3K27me3 Staining

Histologic type	No. of TMA cores (patients, *n*)	Median H3K27me3 intensity	*P* value*	Median H3K27me3 nuclear area ratio	*P* value*	Median H3K27me3 score	*P* value*
Normal/benign							
Normal prostatic epithelium	346 (116)	162.2	NA	0.716	NA	114.16	NA
Atrophy							
Simple atrophy	116 (28)	164	0.11	0.440	<0.0001	71.49	<0.0001
Simple atrophy with cyst formation	4 (4)	176.5	0.13	0.296	0.0143	54.21	0.0280
Post-atrophic hyperplasia	8 (5)	163.2	0.93	0.683	0.1334	107.11	0.2389
Total atrophy	128 (29)	164	0.08	0.454	<0.0001	72.27	<0.0001
PIN							
High grade	61 (22)	154	0.0001	0.655	<0.0001	101.17	0.0174
Mixed high and low grade	7 (6)	155	0.19	0.539	0.0007	80.47	0.0005
Low grade	13 (13)	156	0.02	0.560	0.0064	84.13	0.0010
Total PIN	81 (29)	154.4	0.0001	0.620	0.0015	96.14	0.0004
Carcinoma							
Adenocarcinoma, Gleason 3	64 (45)	147.4	0.0001	0.804	0.0007	113.71	0.8829
Adenocarcinoma, Gleason 4	68 (58)	138.4	0.0001	0.653	0.0774	91.24	<0.0001
Adenocarcinoma, Gleason 5	12 (11)	135.9	0.0001	0.434	0.0053	62.34	0.0006
Total carcinoma	144 (108)	143.4	0.0001	0.733	0.8035	101.36	0.0003
Metastatic carcinoma	67 (67)	138.2	0.0001	0.478	<0.0001	66.26	<0.0001
Total	766 (154)						

Cores with nondiagnostic tissue or cases with only stromal tissue on the TMA spot were not used for the analysis.
*Kruskal-Wallis equality of populations rank test compared to normal prostate epithelium using grouped values.
NA, not applicable.

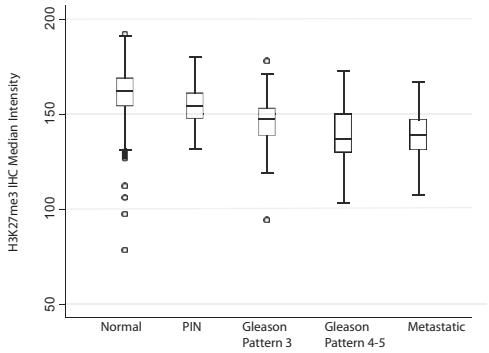

Figure 5. Quantification of immunohistochemistry on TMAs. H3K27me3 levels inversely correlate with worsening disease, in which metastatic and high-grade tumors show the lowest levels of H3K27me3.

Gleason pattern in carcinoma lesions. For example, Gleason pattern 3 tended to show reduced staining intensity as compared to normal epithelium, but not reduced area of nuclear staining, which in fact was significantly higher than normal (Table 2). The median IHC score, which represents a sum of the intensities for cells in a given lesion divided by the total nuclear area, was also not significantly reduced in Gleason pattern 3 adenocarcinoma lesions. Hormone-naive metastatic prostate cancer lesions also show reduced H3K27me3 staining, both in median intensity and area, comparable to that of the higher-grade primary cancer lesions (Figures 4 and 5, Table 2). Staining of a number of prostatic adenocarcinomas for either total H3 or total H3K4me3 revealed no apparent differences between the intensity and area of staining as compared with normal prostatic epithelium (not shown).

H3K27me3 Levels Are Independent of EZH2 Expression in Vivo

EZH2 is known to be overexpressed in prostate cancer. However, by immunofluorescence, we found that levels of H3K27me3 did not correlate with levels of EZH2 in several tissues (see Supplemental Figure S3, A–D, at *http://ajp.amjpathol.org*). The difference was especially noticeable in lymphoid nodules within tonsil tissue, in which there was an apparent inverse correlation between EZH2 and H3K27me3 with minimal colocalization. In the prostate, areas of EZH2 overexpression did not coincidence with areas of high H3K27me3 levels as might be expected. The same, nearly inverse pattern was seen in colon and skin. This observation indicates that levels of H3K27me3 are not linked to EZH2 protein expression.

Regulation of Global Changes in Histone Modifications by MYC

We next examined whether the observed alterations in global H3K27me3 content may be caused by MYC activation, which is known to globally alter heterochromatin states. To examine this *in vivo*, we turned to mice that overexpress MYC in the prostate. Lo-MYC and Hi-MYC mice characteristically develop PIN that progresses to cribriform PIN/intraductal carcinoma and then to localized invasive adenocarcinoma lesions.[16,37] Strikingly, levels of H3K27me3 were markedly reduced in mouse PIN (Figure 2), cribriform PIN, and adenocarcinoma lesions (not shown) as compared to matched normal luminal epithelial cells. These results support the hypothesis that MYC overexpression results in decreases in global H3K27me3 levels in prostatic luminal epithelial cells *in vivo*, concomitant with the morphological appearance of PIN. Further, like their human counterparts, mouse prostatic PIN and carcinomas are characterized by reduced H3K27me3 levels.

To further examine the effects of MYC on global H3K27me3 levels and the potential cell context specificity of its effects, we experimentally manipulated levels of MYC in a number of cancer cell lines. Changes in overall H3K27me3 levels were determined by quantitative Western blotting in which we calculated the normalized ratio of H3K27me3 (normalized to total H3) in cells treated with anti-MYC siRNA to cells treated with a nontargeting scrambled siRNA in the same experiment. In PC3 (androgen receptor–negative prostate cancer cell line) as well as in LNCaP (androgen receptor–positive and androgen-sensitive prostate cancer cell line) cells, MYC knockdown by siRNA resulted in an increase in overall H3K27me3 levels (Figure 6, A–E). Similar results were seen in the MCF7 breast cancer cell line. Further, using a B-cell Burkitt's lymphoma cell line (p493) engineered to silence MYC expression by addition of tetracycline (tet-off cells), H3K27me3 levels were increased after MYC levels were reduced on tetracycline addition (Figure 6E). Interestingly, the effects of MYC levels on global H3K27me3 did not occur in all lines tested; DU145 cells (androgen receptor–negative prostate cancer cell line) did not show increased global levels of H3K27me3 after MYC knockdown (Figure 6F). This was not due to variations in baseline levels of MYC, as DU145 cells and LNCaP show similar levels of MYC (Figure 6E).

Furthermore, to determine whether AR may play a role in LNCaP cells, we manipulated levels of AR with siRNA in the same manner that we manipulated levels of H3K27me3. There was no change in levels of H3K27me3 with changes in levels of AR (see Supplemental Figure S4, A and B, at *http://ajp.amjpathol.org*). Furthermore, we performed immunohistochemistry on C4-2b and CWR22Rv1—castrate-resistant—cell lines as well as the LNCaP—androgen-sensitive—cell line (see Supplemental Figure S5, A–C, at *http://ajp.amjpathol.org*). In this model of prostate cancer progression, the castrate-resistant cell lines did not show altered levels of H3K27me3 as compared to the non–castrate-resistant lines. Therefore, this phenomenon of decreased H3K27me3 levels is independent of AR but not of MYC. Thus, although the effect does not occur in all cells, MYC can induce global changes in levels of H3K27me3 in a number of different cancer cell types, as well as in mouse luminal epithelial cells *in vivo*.

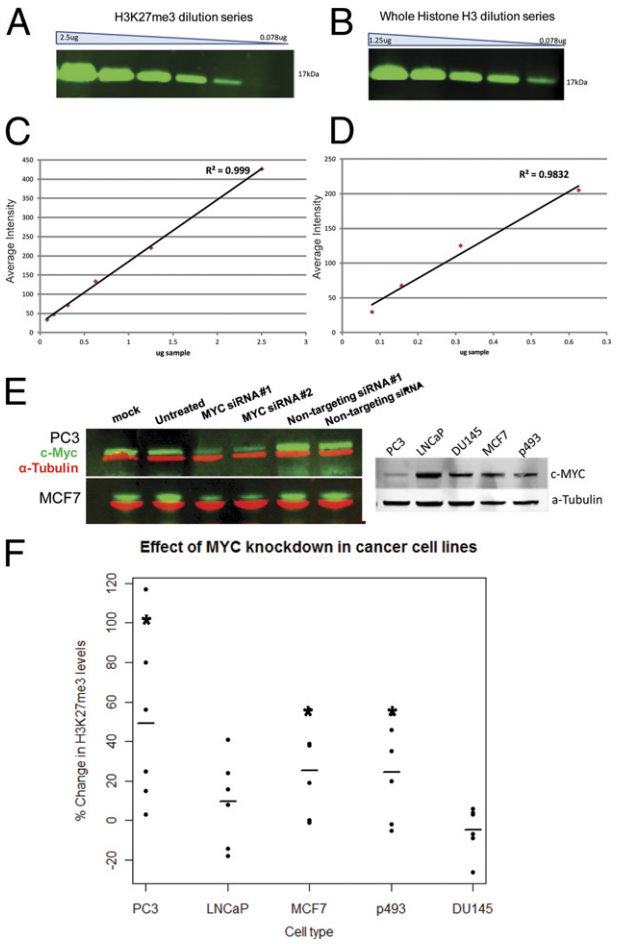

Figure 6. siRNA knockdown of MYC results in increased levels of H3K27me3. A serial dilution series (factor of 2) for H3K27me3 (**A**) and total histone H3 (**B**) with histone protein from PC3 prostate cancer cells show the linear range for each antibody (**C** and **D**) respectively. **E:** Representative Western blots show a siRNA knockdown of MYC protein for two different cell lines as well as baseline levels of MYC in all five cell lines. **F:** MYC knockdown results in increased levels of H3K27me3 in MCF7 (Student's *t*-test, $P < 0.05$), PC3 ($P < 0.05$), p493 ($P = 0.05$), and LNCaP ($P > 0.05$) cell lines, but not in DU145 cells ($P > 0.05$), suggesting the effect is context specific.

Discussion

We report that the normal human and mouse prostates are characterized by increased levels of H3K27me3 in more differentiated luminal cells as compared to the less differentiated stem-like basal cells. This link to the differentiated state of normal cells was also found in a number of other human and rodent tissues that are characterized by rapid tissue renewal and hierarchical differentiation. Further, in both MYC-driven prostate cancers in mice and in clinical human samples, we found that global levels of H3K27me3 are reduced in both PIN and invasive adenocarcinoma lesions. Finally, we showed that in prostate cancer cells, breast cancer cells, and lymphoma cells, experimentally forced reductions in MYC levels resulted in increased global levels of H3K27me3. These results provide: i) evidence that global levels of H3K27me3 are deregulated (eg, reduced) early during prostatic carcinogenesis; ii) evidence that H3K27me3 global levels track with cellular differentiation *in vivo*; iii) evidence that at least one mechanism for H3K27me3 deregulation in prostate and breast cancer results from overexpression of MYC; iv) support for the concept that MYC influences global chromatin structure during the process of neoplastic transformation of prostatic luminal epithelial cells; and v) additional evidence to support the concept that MYC overexpression blocks epithelial cell differentiation in PIN and prostatic adenocarcinomas.[38]

Our main assessment was based on immunohistochemical and immunofluorescent staining. Although it is possible that reduced staining for H3K7me3 in luminal cells of the prostate, PIN, and carcinoma could relate to lack of access to the antibody, it is noteworthy that the cell types that showed a clear differential in staining for H3K27me3 showed no difference in staining for the total H3 protein in multilabel immunofluorescent assays. Since the antibody specificity in Western blots appeared to be very high, we conclude that these results are indicative of lower levels of H3K27me3 in basal cells, PIN cells, and carcinoma cells as compared to normal-appearing luminal cells. Similar results were obtained in both mouse and human tissues, including the difference in basal versus luminal in normal, differentiating cells across many organ systems with hierarchical differentiation, MYC-driven mouse prostate precursors, and invasive lesions.

Although our results suggest that at least one mechanism by which H3K27me3 global levels are regulated involves MYC, it is not clear whether physiological levels of MYC are responsible for the pattern of global H3K27me3 staining observed in normal tissues. This is at least plausible; although we did not examine this question in the current study, it is known that endogenous MYC levels are higher in stem cell compartments of both intestinal epithelium[39] and squamous epithelium of the skin,[40] and MYC levels fall in these tissues as the cells differentiate/mature. Not much is known about the dynamics of global levels of H3K27me3 and normal cellular differentiation. Interestingly, a study that mapped genome-wide occupancy of promoter sites in epidermal keratinocytes found that H3K27me3 marks disappear in a number of epidermal gene promoters concomitant with their induction of expression.[41] However, this study did not examine overall global levels of H3K27me3.

The changes in overall levels of H3K27me3 were quantitatively assessed by Western blot analysis after forced reductions in MYC in cell culture, as well as semiquantitatively by chromogenic IHC and image analysis on tissues. The results of the Western blot studies, which were carefully quantified using assays performed within the linear range, showed an approximately 20% to 50% increase in H3K27me3 levels after MYC knockdown. Interestingly, although IHC is not truly linear, the magnitude of change found by our image analysis of the IHC staining was consistent with those observed in more quantitative Western blots. Intriguingly, Haffner et al[42] recently reported a highly similar pattern of overall staining for 5-hydroxy-methyl cytosine (5-HMC) in human tissues and cancer specimens, suggesting that H3K27me3 and 5-HMC levels may track together.

Our findings might relate to others in terms of oncogene and/or tumor suppressor gene alterations resulting

in global changes in heterochromatin structure as examined here. Transformation of rat fibroblasts by Ras resulted in a less condensed chromatin structure.[15] Further, recent work has shown that loss of the tumor suppressor gene, *BRCA1*, also results in reduced amounts of condensed heterochromatin in both mouse tumors and human cancer cells.[43] Interestingly, loss of *BRCA1* function resulted in derepression and ectopic expression of satellite DNA, and the resultant RNA transcripts lead to DNA damage, cell cycle checkpoint defects, and genomic instability.[43] These findings suggest that decondensation of heterochromatin may be a common feature associated with a number of disparate oncogenic events (eg, Ras activation, MYC overexpression, and *BRCA1* loss). Further, at least in the case of loss of *BRCA1*, this appears to have profound functional relevance in the neoplastic process. Although we have not determined whether MYC overexpression results in derepression of satellite DNA in mouse or human cells, our preliminary data show changes in MYC-induced PIN lesions in the prostate *in vivo* as characterized by widespread reorganization of foci staining for histone H3K9me3, which is known to be associated with DAPI foci (T. Iwata, L. Pellakuru, A.M. De Marzo, unpublished observations). Thus, these results imply that oncogenic alterations in a number of different cancer genes result in alterations in heterochromatin structure, with a general theme emerging of alterations in chromatin condensation in cancer as compared to normal cell counterparts.[15] These pervasive findings in cancer may indeed correlate with changes and increased levels of decondensed chromatin, routinely visualized by anatomic pathologists in diagnostic H & E–stained slides dating back well over 100 years.

Although there is experimental evidence that basal cells are the direct precursor cells for cancer cell formation in the prostate[44] there are other observations and experimental evidence to suggest that intermediate luminal cells, rare stem-like luminal cells called CARNS,[45] or perhaps even mature normal luminal cells can be the targets of transformation in the prostate.[16,19,20,46] In the present study, we found that both basal cells and intermediate cells, which are enriched in regions of focal prostatic atrophy, show reduced H3K27me3 staining as compared to mature luminal cells. Although these results do not shed light on the cell of origin *per se*, it is of interest that basal cells and intermediate cells, which are both clearly less differentiated than luminal cells (eg, less AR, NKX3.1, PSA in humans, etc), share the feature of reduced H3K27me3 with PIN cells (which have a luminal-like phenotype) and prostate cancer cells.

Our findings raise a number of interesting questions that require additional clarification in future studies. For example, since MYC overexpression also causes up-regulation of EZH2,[30] and EZH2 is up-regulated in prostate cancer and other cancers, it is currently unclear why global levels of H3K27me3 are decreased by MYC overexpression and decreased in prostate cancer and PIN. A recent report by Hyland et al[47] indicated that transduction of keratinocytes transduced with human papillomavirus type-16 E6/E7 genes resulted in an increase in EZH2 levels and a decrease in global levels of H3K27me3. These authors suggested that whereas EZH2 protein was overexpressed, as a result of increased phosphorylation of serine 21 on EZH2, there was likely reduced EZH2 methyltransferase activity. Hyland et al found down-regulation of PRC1 components, as well as increased levels of KDM6A, a histone lysine demethylase, all of which can lead to reduced H3K27me3. Finally, in human squamous intraepithelial neoplasia, a precursor to invasive squamous cell carcinoma, there were reduced levels of H3K27me3,[47] similar to what we report here in PIN lesions. Although we have recently shown that MYC overexpression in prostate cancer results in increased EZH2 mRNA and protein levels, we did not measure EZH2 histone lysine methyltransferase activity or phosphorylation of serine 21 of EZH2.[30] We performed immunohistochemistry on various tissues, and we show that levels of H3K27me3 do not vary directly with EZH2; in fact, they seem to vary inversely as can been seen clearly in tonsil. In other tissues, there is very little coexpression of EZH2 and H3K27me3, indicating that levels of H3K27me3 may be independent of EZH2 expression, supporting the conclusions of Hyland et al. Thus, the precise mechanisms by which MYC overexpression leads to decreased global levels of H3K27me3 await future studies, including whether MYC affects expression or activity of histone 3 lysine 27 demethylases in prostate cancer. Another question is what is the nature of the context-specific finding whereby forced reductions of MYC result in increased H3K27me3 levels in some prostate cancer and breast cancer cells, but not in other prostate cancer cells *in vitro*? What functional modules of MYC protein are required for affecting H3K27me3 levels? What other histone marks are affected by MYC in a global fashion in prostate cancer and PIN cells? How do these findings of reduced levels of a repressive histone mark correlate with previously reported reduced levels of a number of histone activation marks in prostate cancer?[48]

In summary, we show that a key marker of at least some types of heterochromatin, the polycomb repressive mark, H3K27me3, increases in many lineages *in vivo* as cells differentiate. Further, H3K27me3 is markedly reduced in prostate cancer cells, and this reduction occurs at the precursor lesion stage in prostate cancer (eg, PIN), correlates with markers of disease aggressiveness, is retained into advanced phases of the disease, and is regulated at least in part by MYC. These studies provide potential new mechanistic insights into a long-standing observation whereby PIN and prostate cancer cells show widespread decondensation of chromatin.

Acknowledgments

We thank Helen Fedor, Marcela Southerland, Kristen Lecksell, and the Brady Urological Institute Prostate Specimen Repository for fresh prostate tissues and tissue microarrays and Donald S. Coffey for careful reading of the manuscript and helpful suggestions.

References

1. Meyer N, Penn LZ: Reflecting on 25 years with MYC. Nat Rev Cancer 2008, 8:976–990
2. Cartwright P, McLean C, Sheppard A, Rivett D, Jones K, Dalton S: LIF/STAT3 controls ES cell self-renewal and pluripotency by a Myc-dependent mechanism. Development 2005, 132:885–896
3. Varlakhanova NV, Cotterman RF, deVries WN, Morgan J, Donahue LR, Murray S, Knowles BB, Knoepfler PS: myc maintains embryonic stem cell pluripotency and self-renewal. Differentiation 2010, 80:9–19
4. Jaenisch R, Young R: Stem cells, the molecular circuitry of pluripotency and nuclear reprogramming. Cell 2008, 132:567–582
5. Takahashi K, Tanabe K, Ohnuki M, Narita M, Ichisaka T, Tomoda K, Yamanaka S: Induction of pluripotent stem cells from adult human fibroblasts by defined factors. Cell 2007, 131:861–872
6. Wong DJ, Liu H, Ridky TW, Cassarino D, Segal E, Chang HY: Module map of stem cell genes guides creation of epithelial cancer stem cells. Cell Stem Cell 2008, 2:333–344
7. Kim J, Woo AJ, Chu J, Snow JW, Fujiwara Y, Kim CG, Cantor AB, Orkin SH: A Myc network accounts for similarities between embryonic stem and cancer cell transcription programs. Cell 2010, 143:313–324
8. Rothenberg ME, Clarke MF, Diehn M: The Myc connection: eS cells and cancer. Cell 2010, 143:184–186
9. Varlakhanova NV, Knoepfler PS: Acting locally and globally: myc's ever-expanding roles on chromatin. Cancer Res 2009, 69:7487–7490
10. Gaspar-Maia A, Alajem A, Meshorer E, Ramalho-Santos M: Open chromatin in pluripotency and reprogramming. Nat Rev Mol Cell Biol 2011, 12:36–47
11. Knoepfler PS, Zhang XY, Cheng PF, Gafken PR, McMahon SB, Eisenman RN: Myc influences global chromatin structure. EMBO J 2006, 25:2723–2734
12. Martinato F, Cesaroni M, Amati B, Guccione E: Analysis of Myc-induced histone modifications on target chromatin. PLoS One 2008, 3:e3650
13. Cotterman R, Jin VX, Krig SR, Lemen JM, Wey A, Farnham PJ, Knoepfler PS: N-Myc regulates a widespread euchromatic program in the human genome partially independent of its role as a classical transcription factor. Cancer Res 2008, 68:9654–9662
14. Zink D, Fischer AH, Nickerson JA: Nuclear structure in cancer cells. Nat Rev Cancer 2004, 4:677–687
15. Easwaran HP, Baylin SB: Role of nuclear architecture in epigenetic alterations in cancer. Cold Spring Harb Symp Quant Biol 2010, 75: 507–515
16. Iwata T, Schultz D, Hicks J, Hubbard GK, Mutton LN, Lotan TL, Bethel C, Lotz MT, Yegnasubramanian S, Nelson WG, Dang CV, Xu M, Anele U, Koh CM, Bieberich CJ, De Marzo AM: MYC overexpression induces prostatic intraepithelial neoplasia and loss of Nkx3.1 in mouse luminal epithelial cells. PLoS One 2010, 5:e9427
17. Allam CK, Bostwick DG, Hayes JA, Upton MP, Wade GG, Domanowski GF, Klein MA, Boling EA, Stilmant MM: Interobserver variability in the diagnosis of high-grade prostatic intraepithelial neoplasia and adenocarcinoma. Mod Pathol 1996, 9:742–751
18. Bostwick DG, Pacelli A, Lopez-Beltran A: Molecular biology of prostatic intraepithelial neoplasia. Prostate 1996, 29:117–134
19. Gurel B, Iwata T, Koh CM, Jenkins RB, Lan F, Van Dang C, Hicks JL, Morgan J, Cornish TC, Sutcliffe S, Isaacs WB, Luo J, De Marzo AM: Nuclear MYC protein overexpression is an early alteration in human prostate carcinogenesis. Mod Pathol 2008, 21:1156–1167
20. Koh CM, Bieberich CJ, Dang CV, Nelson WG, Yegnasubramanian S, De Marzo AM: MYC and prostate cancer. Genes Cancer 2010, 1:617–628
21. Nikoloski G, Langemeijer SM, Kuiper RP, Knops R, Massop M, Tonnissen ER, van der Heijden A, Scheele TN, Vandenberghe P, de Witte T, van der Reijden BA, Jansen JH: Somatic mutations of the histone methyltransferase gene EZH2 in myelodysplastic syndromes. Nat Genet 2010, 42:665–667
22. Sauntharajah Y, Maciejewski J: Polycomb segment myeloid malignancies. Blood 2012, 119:1097–1098
23. Martinez-Garcia E, Licht JD: Deregulation of H3K27 methylation in cancer. Nat Genet 2010, 42:100–101
24. McCabe MT, Graves AP, Ganji G, Diaz E, Halsey WS, Jiang Y, Smitheman KN, Ott HM, Pappalardi MB, Allen KE, Chen SB, Della Pietra A 3rd, Dul E, Hughes AM, Gilbert SA, Thrall SH, Tummino PJ, Kruger RG, Brandt M, Schwartz B, Creasy CL: Mutation of A677 in histone methyltransferase EZH2 in human B-cell lymphoma promotes hypertrimethylation of histone H3 on lysine 27 (H3K27), Proc Natl Acad Sci U S A 2012, 109:2989–2994
25. Chase A, Cross NC: Aberrations of EZH2 in cancer. Clin Cancer Res 2011, 17:2613–2618
26. Varambally S, Dhanasekaran SM, Zhou M, Barrette TR, Kumar-Sinha C, Sanda MG, Ghosh D, Pienta KJ, Sewalt RGAB, Otte AP, Rubin MA, Chinnaiyan AM: The polycomb group protein EZH2 is involved in progression of prostate cancer. Nature 2002, 419:624–629
27. Kleer CG, Cao Q, Varambally S, Shen RL, Ota L, Tomlins SA, Ghosh D, Sewalt RGAB, Otte AP, Hayes DF, Sabel MS, Livant D, Weiss SJ, Rubin MA: EZH2 is a marker of aggressive breast cancer and promotes neoplastic transformation of breast epithelial cells. Proc Natl Acad Sci U S A 2003, 100:11606–11611
28. Bryant RJ, Cross NA, Eaton CL, Hamdy FC, Cunliffe VT: EZH2 promotes proliferation and invasiveness of prostate cancer cells. Prostate 2007, 67:547–556
29. Karanikolas BD, Figueiredo ML, Wu L: Polycomb group protein enhancer of zeste 2 is an oncogene that promotes the neoplastic transformation of a benign prostatic epithelial cell line. Mol Cancer Res 2009, 7:1456–1465
30. Koh CM, Iwata T, Zheng Q, Bethel C, Yegnasubramanian S, De Marzo AM: Myc enforces overexpression of EZH2 in early prostatic neoplasia via transcriptional and post-transcriptional mechanisms. Oncotarget 2011, 2:669–683
31. Shi B, Liang J, Yang X, Wang Y, Zhao Y, Wu H, Sun L, Zhang Y, Chen Y, Li R, Hong M, Shang Y: Integration of estrogen and Wnt signaling circuits by the polycomb group protein EZH2 in breast cancer cells. Mol Cell Biol 2007, 27:5105–5119
32. Rogenhofer S, Kahl P, Mertens C, Hauser S, Hartmann W, Buttner R, Muller SC, von Ruecker A, Ellinger J: Global histone H3 lysine 27 (H3K27) methylation levels and their prognostic relevance in renal cell carcinoma. BJU Int 2012, 109:459–465
33. Wei Y, Xia W, Zhang Z, Liu J, Wang H, Adsay NV, Albarracin C, Yu D, Abbruzzese JL, Mills GB, Bast RC Jr., Hortobagyi GN, Hung M-C: Loss of trimethylation at lysine 27 of histone H3 is a predictor of poor outcome in breast, ovarian, and pancreatic cancers. Mol Carcinog 2008, 47:701–706
34. Lawson DA, Zong Y, Memarzadeh S, Xin L, Huang J, Witte ON: Basal epithelial stem cells are efficient targets for prostate cancer initiation. Proc Natl Acad Sci U S A 2010, 107:2610–2615
35. Garraway IP, Sun W, Tran CP, Perner S, Zhang B, Goldstein AS, Hahm SA, Haider M, Head CS, Reiter RE, Rubin MA, Witte ON: Human prostate sphere-forming cells represent a subset of basal epithelial cells capable of glandular regeneration in vivo, Prostate 2010, 70:491–501
36. De Marzo AM, Platz EA, Sutcliffe S, Xu J, Gronberg H, Drake CG, Nakai Y, Isaacs WB, Nelson WG: Inflammation in prostate carcinogenesis. Nat Rev Cancer 2007, 7:256–269
37. Ellwood-Yen K, Graeber TG, Wongvipat J, Iruela-Arispe ML, Zhang J, Matusik R, Thomas GV, Sawyers CL: Myc-driven murine prostate cancer shares molecular features with human prostate tumors. Cancer Cell 2003, 4:223–238
38. Koh CM, Gurel B, Sutcliffe S, Aryee MJ, Schultz D, Iwata T, Uemura M, Zeller KI, Anele U, Zheng Q, Hicks JL, Nelson WG, Dang CV, Yegnasubramanian S, De Marzo AM: Alterations in nucleolar structure and gene expression programs in prostatic neoplasia are driven by the MYC oncogene. Am J Pathol 2011, 178:1824–1834
39. van de Wetering M, Sancho E, Verweij C, de Lau W, Oving I, Hurlstone A, van der Horn K, Batlle E, Coudreuse D, Haramis AP, Tjon-Pon-Fong M, Moerer P, van den Born M, Soete G, Pals S, Eilers M, Medema R, Clevers H: The beta-catenin/TCF-4 complex imposes a crypt progenitor phenotype on colorectal cancer cells. Cell 2002, 111:241–250
40. Hurlin PJ, Foley KP, Ayer DE, Eisenman RN, Hanahan D, Arbeit JM: Regulation of Myc and Mad during epidermal differentiation and HPV-associated tumorigenesis. Oncogene 1995, 11:2487–2501
41. Sen GL, Webster DE, Barragan DI, Chang HY, Khavari PA: Control of differentiation in a self-renewing mammalian tissue by the histone demethylase JMJD3. Genes Dev 2008, 22:1865–1870
42. Haffner MC, Chaux A, Meeker AK, Esopi DM, Gerber J, Pellakuru LG, Toubaji A, Argani P, Iacobuzio-Donahue C, Nelson WG, Netto GJ, De Marzo AM, Yegnasubramanian S: Global 5-hydroxymethylcytosine

content is significantly reduced in tissue stem/progenitor cell compartments and in human cancers. Oncotarget 2011, 2:627–637
43. Zhu Q, Pao GM, Huynh AM, Suh H, Tonnu N, Nederlof PM, Gage FH, Verma IM: BRCA1 tumour suppression occurs via heterochromatin-mediated silencing. Nature 2011, 477:179–184
44. Goldstein AS, Huang J, Guo C, Garraway IP, Witte ON: Identification of a cell of origin for human prostate cancer, Science 2010, 329:568–571
45. Wang X, Kruithof-de Julio M, Economides KD, Walker D, Yu H, Halili MV, Hu YP, Price SM, Abate-Shen C, Shen MM: A luminal epithelial stem cell that is a cell of origin for prostate cancer, Nature 2009, 461:495–500
46. De Marzo AM, Nelson WG, Bieberich CJ, Yegnasubramanian S: Prostate cancer: new answers prompt new questions regarding cell of origin. Nat Rev Urol 2010, 7:650–652
47. Hyland PL, McDade SS, McCloskey R, Dickson GJ, Arthur K, McCance DJ, Patel D: Evidence for alteration of EZH2, BMI1, and KDM6A and epigenetic reprogramming in human papillomavirus type 16 E6/E7-expressing keratinocytes, J Virol 2011, 85:10999–11006
48. Seligson DB, Horvath S, Shi T, Yu H, Tze S, Grunstein M, Kurdistani SK: Global histone modification patterns predict risk of prostate cancer recurrence. Nature 2005, 435:1262–1266